Delft University of Technology

Effects of thermal hydrolysis process-generated melanoidins on partial nitritation/anammox in full-scale installations treating waste activated sludge

Pavez-Jara, Javier A.; van Lier, Jules B.; de Kreuk, Merle K.

Important note
To cite this publication, please use the final published version (if applicable).
Please check the document version above.

Effects of thermal hydrolysis process-generated melanoidins on partial nitritation/anammox in full-scale installations treating waste activated sludge

Javier A. Pavez-Jara [*], Jules B. van Lier, Merle K. de Kreuk

Department of Water Management, Delft University of Technology, Building 23 Stevinweg 1, 2628, Delft, the Netherlands

ABSTRACT

Thermal hydrolysis process (THP) is a well-established anaerobic digestion (AD) pre-treatment technology. Despite the THP benefits the pre-treatment increases the concentrations of nutrients and melanoidins in the digestate reject water after dewatering. The increased concentrations of nutrients and melanoidins formed during THP-AD can impact downstream processes, such as struvite precipitation and partial nitritation/anammox (PN/A). In our present work, six full-scale PN/A influents and effluents were sampled in The Netherlands (4 with THP and 2 without THP). Full-scale samples were characterised and the stoichiometric O_2 consumption and melanoidins chelated to trace elements were analysed. The results showed that THP increased the concentration of total ammoniacal nitrogen (TAN), chemical oxygen demand (COD), total organic carbon (TOC), UVA 254 and colour, which are indicators of melanoidins occurrence. THP furthermore decreased the stoichiometric NO_3^--N production from the PN/A reaction in effluents. The disparity between stoichiometric and measured NO_3^--N in the THP-using plants was explained by the proliferation of denitrifiers. Moreover, denitrification improved the N removal efficiency due to the consumption of the stoichiometrically-produced NO_3^--N. Also, the stoichiometric O_2 consumption increased in the plants using THP, reaching up to 56% of the O_2 used for partial oxidation of TAN. Trace elements analysis revealed that the plants with elevated concentrations of melanoidins in the effluent showed a high percentage of chelated multivalent cations, particularly transition metals such as Fe. Kendall correlation coefficient analysis showed that the chelation of multivalent cations was correlated mainly with colour occurrence in the reject waters. Overall, the results indicated that in PN/A systems using THP-AD increased O_2 consumption and trace elements availability should be considered during the process design.

1. Introduction

Anaerobic digestion (AD) is a well-established technology to diminish the amount of excess sludge from wastewater treatment plants (WWTPs) and to recover biochemical energy as biogas (Appels et al., 2008). During AD of primary and secondary sludges, hydrolysis of particulate matter determines the overall conversion rate of the process, and is thus considered the "rate-limiting step" (Appels et al., 2008; Pavlostathis and Giraldo-Gomez, 1991; Tiehm et al., 2001). Hydrolysis acceleration has been reached at both lab-scale and full-scale by the application of pre-treatments on the AD substrates (Appels et al., 2008; Hendriks and Zeeman, 2009). Thermal hydrolysis process (THP) is the most widespread pre-treatment for AD; it has become commercially available in Norway in the 1990s, and has since expanded to the rest of

the world (Devos et al., 2023; Kor-Bicakci and Eskicioglu, 2019; Ødeby et al., 1996). During THP, the AD substrates' temperature is increased to 140–170 °C for around 20–30 min, followed by a sudden decrease in pressure (and temperature), which causes cell disruption and cytoplasmic content release (Ringoot et al., 2012). The use of THP-AD has demonstrated advantages such as reduced pathogens concentrations in AD effluents, increased anaerobic biodegradability, and improved mixing and dewaterability of the AD-digestates (Barber, 2016). Despite the evident advantages of THP, it has been observed that this pre-treatment increases nutrient concentrations and leads to the formation of recalcitrant compounds (Dwyer et al., 2008b).

THP-AD systems are characterised by increased total ammoniacal nitrogen (TAN) concentrations as a consequence of increased solubilisation and biodegradability of proteins (Bougrier et al., 2008; Li and

Noike, 1992). The increased nutrients solubilisation in THP-AD can lead to negative effects in the AD process, such as free ammonia nitrogen (FAN) inhibition and spontaneous struvite precipitation (Barber, 2016; Yuan et al., 2012). Additionally, elevated nutrients concentrations can affect AD downstream processes as follows: 1) Increased Mg^{2+} requirements in struvite precipitation due to increased PO_4^{3-} concentrations, which may increase PO_4^{3-} recovery, and 2) Increased O_2 requirements to convert elevated TAN concentrations into N_2 in mainstream conventional nitrification-denitrification processes or a partial nitration-anammox (PN/A) process in the reject water line. Furthermore, Zhang, T. et al. (2020) observed that PO_4^{3-} increased along with the THP pre-treatment temperature and with reaction times shorter than 30 min. PO_4^{3-} release can be attributed to the disintegration of phosphate-accumulating organisms (PAOs) present in waste activated sludge (WAS) from WWTPs using enhanced biological phosphorous removal (Coats et al., 2011; Qiu et al., 2019). Also, the presence of living PAOs during AD can lead to increased PO_4^{3-} concentrations as a result of their VFA uptake accompanied by PO_4^{3-} release (Flores-Alsina et al., 2016; Wang et al., 2016). However, PO_4^{3-} solubility in the AD reactors' digestates depends on the cationic load among other factors (e.g. pH and reagent concentrations), which determine the precipitation of P-based minerals (Flores-Alsina et al., 2016). In increasing numbers of full-scale installations, soluble PO_4^{3-} in AD reject water is removed using the struvite precipitation process, in which Mg^{2+} is added at mildly elevated pH. However, during struvite precipitation other P-based minerals can co-precipitate with different metals such as Al^{3+}, Ca^{2+}, and $Fe^{2+/3+}$ (Becker et al., 2019; Fischer et al., 2011).

In addition to the increased nutrients concentrations, THP leads to the formation of melanoidins, which are coloured polymers from the Maillard reaction (Dwyer et al., 2008b; Penaud et al., 2000). Melanoidins are formed when carbohydrates and proteins are exposed to high temperatures, leading to polymerisation reactions and thus increased molecular weight and a higher degree of aromaticity (Hodge, 1953; Wang et al., 2011). Like humic substances (HSs) and irrespective their anthropogenic origin, melanoidins can be classified as fulvic acids, humic acids and humins, depending on their pH-dependent solubility (L. Malcolm, 1990; McDonald et al., 2004; Migo et al., 1993). Melanoidins furthermore behave as polydentate ligands, chelating ions in solution in the same way as conventional HSs. The complexing effect of HSs has been widely used in agriculture to chelate nutrients, and promote their slow release (El-sayed et al., 2017; Morales et al., 2005). As a result of the complex chemical composition of THP-formed melanoidins, part of these compounds cannot be anaerobically biodegraded, and reach the AD downstream processes.

After THP-AD, the reject water contains an elevated concentration of nutrients, which is increasingly removed prior conveying the reject water to the headworks of the WWTP to safeguard its proper functioning. A common option to remove TAN in reject waters is the PN/A process, which is less expensive compared to the traditional nitrification/denitrification process in the WWTP's mainstream. Compared to nitrification/denitrification, PN/A requires 50–60 % less O_2 consumption and it does not require any organic matter as electron donor for the ultimate denitrification step (Fux and Siegrist, 2004). The PN/A process was discovered and further developed in the 1990s and has been growing thenceforth to reach over a hundred full-scale plants operating in 2014 (Lackner et al., 2014). As the name suggests, PN/A reactors work in a dynamic equilibrium between two main microbial populations: 1) aerobic ammonium oxidising organisms (AOO) and 2) anoxic ammonium oxidisers (anammox) (Gilbert et al., 2013; Lotti et al., 2014a). In a simplified way, AOO use O_2 to convert NH_4^+ into NO_2^-, and anammox microorganisms oxidise NH_4^+ using NO_2^- to produce N_2. After the N_2 concentration reaches saturation in the liquid, N_2 is stripped to the gas phase (Baeten et al., 2019; Strous et al., 1998; Van Hulle et al., 2010). Since modern PN/A systems comprise only one single-step reactor, AOO and anammox microorganisms coexist in a delicate equilibrium, conducting their metabolic reactions in parallel (Lackner et al.,

2014). Moreover, PN/A reactors treating reject waters from the AD process, make beneficial use of the high TAN concentrations, high temperature (30–35 °C), and low organics concentrations (Joss et al., 2009). However, THP modifies the properties of reject water and the subsequent PN/A process' influent. Furthermore, organics formed during THP-AD can cause diffusional limitation on the AOO, hindering the PN/A process (Zhang, Q. et al., 2018). Also, the THP-formed organic matter in reject water may imbalance the microbial populations in PN/A, leading to the growth of heterotrophs (Wang et al., 2020). In addition, the heterotrophic degradation of THP-produced melanoidins using O_2 might lead to elevated O_2 uptake rates in the PN/A reactors. Furthermore, the melanoidin's-mediated cations complexation may cause a scarcity of available trace elements, which might hinder the growth of the PN/A microbial populations.

In our present work, we researched the observed performance differences between PN/A reactors treating reject waters from anaerobic digesters fed with THP pre-treated sludge versus and digesters fed with non-pre-treated sludge. To better understand the impact of THP pre-treatment on the PN/A process, the biomass, nutrients, organics, and soluble cations were characterised and compared between the PN/A reactors treating either THP-treated sludge reject water or reject water without pre-treatment. In addition, stoichiometric calculations were performed to assess the aerobic/anoxic biodegradability of the (semi) recalcitrant organics produced during THP (melanoidins), using different final electron acceptors. The latter, permits analysis of whether denitrification occurred as a possible N-removal pathway. Finally, trace elements complexation assays were conducted to investigate trace metals availability and the possible occurrence of microbial growth factors limitations in the full-scale PN/A reactors.

2. Methodology

2.1. Sampling campaign in full-scale PN/A reactors

Influent and effluent from side stream PN/A processes treating AD-reject water were sampled in six WWTPs, all located in the Netherlands. The PN/A effluent samples included homogenous samples containing liquid broth and biomass. Only one sample was taken, and the measured values correspond to that sampling moment. The locations and some process characteristics of the studied WWTPs are shown in Table 1. After the sampling, the biomass and reject waters were stored separately at 4 °C for further analysis.

2.2. Chemical analysis

True colour was determined in 0.45 μm filtered samples, using filters CHROMAFIL Xtra PES-45/25 (Macherey-Nagel, Germany). The absorbance was measured at 475 nm using a Platinum–Cobalt colour standard solution (Hazen 500, Certipur® Merck, Germany) with a concentration of 500 mg Pt-Co/L, in a Genesys 10S UV–Vis spectrophotometer (Thermo Scientific, USA), using 1 cm pathway plastic cuvettes. UVA 254 was measured in filtered samples in the same spectrophotometer as true colour at 254 nm using 1 cm pathway quartz cuvettes. The results are expressed in mg Pt-Co/L and 1/cm in the case of T. colour and UVA 254, respectively. Specific ultraviolet absorbance (SUVA) was calculated as the quotient among UVA 254 in metres, and total organic carbon (TOC) in mg/L.

Total and volatile solids (TS and VS, respectively) were measured according to Standard methods for the examination of water and wastewater (Rice et al., 2012), when measuring TS and VS in granular biomass, the samples were first crushed to homogenise them. Chemical oxygen demand (COD), TOC, ortho and total phosphate (PO_4^{3-}-P and TP, respectively), TAN, NO_2^--N, NO_3^--N, and total-N (TN) were measured with the Hach Lange kits LCK114, LCK386, LCK350, APC303, LCK342, LCK340 and LCK338, respectively (Hach, USA). Electroconductivity (EC) was measured with a probe LF 413T IDS (Xylem, Germany).

Table 1
Characteristics of the WWTPs sampled in our study.

	Sluisjesdijk (SLU)	Olburgen (OLB)	Tilburg (TIL)	Hengelo (HEN)	Apeldoorn (APE)	Amersfoort (AME)
THP system (if applies)	No THP	No THP	CAMBI®	CAMBI®	TURBOTEC ® SUSTEC	LYSOTERM® ELIQUO WATER & ENERGY BV
PN/A system	Two steps SHARON/ ANAMMOX ®	CANNON ®	ANAMMOX ®	NAS-ONE ® COLSEN	DEMON ®	DEMON ®
Influent origin	Municipal AD reject water sampled after struvite precipitation.	Combined anaerobically treated potato starch wastewater + municipal AD reject water sampled after struvite precipitation.	Municipal AD reject water sampled after struvite precipitation.	Municipal AD reject water sampled after struvite precipitation.	Municipal AD reject water sampled after struvite precipitation.	Municipal AD reject water sampled after struvite precipitation.

Volatile fatty acids (VFA) were measured using gas chromatography coupled with a flame ionisation detector (FID-GC) (Shimadzu GC 14B, Japan) following the description of (Ceron-Chafla et al., 2020). The samples were measured in triplicate, and the error bars' length in the results represents two times the standard deviation among the measurements.

2.3. Metals concentration measurements in the analysed PN/A reactors

The soluble concentrations of B, Na, Mg, Al, K, Ca, Mn, Fe, Co, Ni, Cu, Zn, Mo and Cd in the studied samples were measured using ICP-MS (PlasmaQuant MS, Analytik Jena AG, Germany). The samples for ICP-MS analysis were prepared acidifying 9.9 mL of 0.22 µm filtered samples using 0.1 mL of HNO_3 69% (CAS No.: 7697-37-2, CARL ROTH ROTIPURAN ®, Germany). The parameters used in the ICP-MS device are shown in additional information. ICP-MS measures the total concentration of the analysed isotopes, thus the concentrations of the measured cations are expressed without their oxidation state, although they are likely ionised in solution.

2.4. Melanoidins-metals complexation assays using ultrafiltration

Bioavailability of trace elements is a complicated parameter to measure. However, we assumed that the non-bound metals were more bioavailable than the complexed ones. To measure the complexation of multiple metals with melanoidins at the same time, the full-scale samples were fractioned using crossflow ultrafiltration membranes to reject the high molecular weight compounds that behave as multidentate ligands. The membranes used to conduct the fractionation were a nominal 0.5 µm glass fibre filter Advantec GC-50 (Frisenette, Denmark) and a 1 kDa Ultracel® regenerated cellulose membrane (Merck Millipore, USA). The fractionation was conducted using an Amicon ® stirred cell Model 8010 (Merck Millipore, USA) at 21 ± 2 °C using Ar gas at 2.8 bar to induce the trans-membrane pressure, and 600 rpm stirring speed to minimise the cake/gel layer formation. After the micro- and ultra-filtrations, the samples were characterised, measuring COD, TOC, Colour, UVA 254 (supplementary material Figure A1) and metals concentrations in both fractions. Metals in the analysed samples were measured using ICP-MS. The results are expressed as concentration, and as the quotient of the concentration of each cation in the 1 kDa permeate over the concentration in the 0.5 µm permeate.

2.5. Biomass specific substrates conversion rates

To measure the microbial activity in the analysed PN/A reactors, we measured specific ammonium oxidising activity (SAOA), specific anammox activity (SAA) and specific denitrifying activity (SDA) in batch tests. The culture media used to measure the microbial activities are shown in supplementary information. In all the specific activity measurements, flocs and granules were taken as homogeneously as possible from the samples to resemble the full-scale conditions.

Furthermore, to avoid possible inhibition from the melanoidins/substrate still present in the sample broths, the PN/A biomass was rinsed before performing the activity tests. The rinsing was performed using the same culture medium in which the respective activity was measured without adding the respective substrates. The biomass was rinsed three times doubling the samples' volume, followed by soft centrifugation at 3500 rpm for 10 min, in a centrifuge model Heraeus Labofuge 400 (Thermo Fisher Scientific, USA). Since the analysed samples contained granular biomass, the solids concentration could not be determined beforehand, and was estimated based on previous tests before conducting the activity measurement. After each activity measurement was completed, the biomass used was crushed and the actual VS concentration was measured and used to calculate the activity value in gN/gVS/day.

SAOA was measured respirometrically at 35 ± 1 °C in a 120 mL stirred and sealed reaction chamber, connected to a dissolved oxygen (DO) probe model FDO® 925 (WTW, Germany) (additional material, Figure A1). Initially, the vessel containing the culture medium without substrate was magnetically stirred keeping the upper valve open (valve 1 in Figure A1, additional material) to allow air exchange and reach DO saturation. After DO reached the saturation concentration, the previously rinsed PN/A biomass was added to the reaction chamber, which was filled with the culture medium without substrate, and the upper valve was closed. A 20X concentrated TAN solution was added to the culture medium through the lower valve (valve 2 in Figure A1, additional material) to start the reaction. The reaction was stopped when the DO concentration reached 3 mg O_2/L, and the maximum slope of the DO depletion curve was transformed stoichiometrically to N consumed per day, per VS, and was used as the activity indicator.
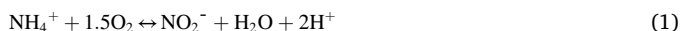
SAA and SDA were determined manometrically using an Oxytop® IS system (WTW, Germany) in triplicate, measuring the overpressure generated by the N_2 produced as a result of the anammox and/or denitrification reactions. SAA and SDA were determined using sealed bottles with 200 mL of reaction volume and around 130 mL of headspace. The exact volume of each bottle was determined in advance. In the same way as in all the activity measurements, the biomass was washed with their respective culture medium without substrate to remove the residual reject water that might interfere with the measurements. Before starting the measurements, the culture medium without substrate and the biomass were flushed for 1 min with Ar gas, and the samples were placed on a stirring plate and warmed until they reached 35 °C in a temperature-controlled incubator. After the constant temperature was reached, the inner pressure was equalised to atmospheric, and the concentrated substrate(s) were added with a syringe. The moles of N_2 produced were calculated using the ideal gas law, Henry's constant at 35 °C (for dissolved N_2) and a correction factor from Antoine's law at 35 °C, which considers that 5.54 % of the total pressure in the headspace corresponds to water vapour. After the specific activity was completed, the headspace gas composition was measured, and the biomass was crushed to take homogenous samples for VS measurement. The specific activity measurement was considered as the maximum

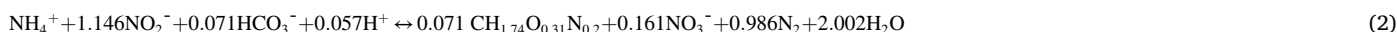slope of the N$_2$ production curve over the mass of biomass (VS) and time.

2.6. Stoichiometric calculations

Stoichiometric NO$_3^-$-N productions in the reactors analysed were calculated according to Equation (3), based on the anammox conversion reaction reported by Lotti et al. (2014b).
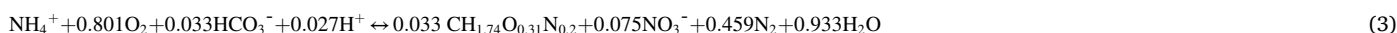
Partial nitritation:

$$NH_4^+ + 1.5O_2 \leftrightarrow NO_2^- + H_2O + 2H^+ \tag{1}$$

Anammox:

$$NH_4^+ + 1.146NO_2^- + 0.071HCO_3^- + 0.057H^+ \leftrightarrow 0.071\,CH_{1.74}O_{0.31}N_{0.2} + 0.161NO_3^- + 0.986N_2 + 2.002H_2O \tag{2}$$

Partial nitritation and anammox:

$$NH_4^+ + 0.801O_2 + 0.033HCO_3^- + 0.027H^+ \leftrightarrow 0.033\,CH_{1.74}O_{0.31}N_{0.2} + 0.075NO_3^- + 0.459N_2 + 0.933H_2O \tag{3}$$

Equation (4) shows the theoretical NO^{3-}-N that should be found in the PN/A reactors effluents, based on TAN concentrations and the stoichiometric calculations shown in Equation (3).

$$NO_3^--N_{theoretical} = 0.075\,\frac{gNO_3^--N}{gTAN}\,(TAN_{influent}-TAN_{effluent}) \tag{4}$$

If it is assumed that the overall volume in the influent and effluent are equal, the NO$_3^-$-N produced can be calculated as the difference between the concentration in the effluent and the influent, as shown in Equation (5).

$$NO_3^--N_{produced} = (NO_3^--N_{effluent}-NO_3^--N_{influent}) \tag{5}$$

To calculate the required amount of electrons to denitrify NO$_3^-$-N to N$_2$, Equation (6) was used. In the case of TIL and HEN the NO$_3^-$-N concentration in the effluent was slightly lower than in the influent thus the variation in those cases was considered equal to zero to avoid negative values.

Denitrification:

$$NO_3^- + 5e^- + 6\,H^+ \leftrightarrow 0.5\,N_2 + 3\,H_2O \tag{6}$$

From Equation (6) the organic matter (COD) that can be oxidised using NO$_3^-$-N as final electron acceptor was calculated, and it is shown in Equation (7).

$$\frac{COD}{NO_3^--N} = 2.857\,\frac{gCOD}{gNH_3^--N}\,NO_3^--N_{produced} \tag{7}$$

To quantify the (extra)oxygen consumptions in the analysed reactors, the indexes shown in Equations (8)–(10) were calculated. Equation (8) shows The NO$_3^-$-N used to oxidise organic matter present in the PN/A reactors via denitrification, expressed as COD according to Equation (7). Equation (9) shows the O$_2$ used to oxidise organic matter present in the PN/A reactors. Finally, Equation (10) shows the O$_2$ used to partially oxidise TAN.

$$NO_3^--N_{Ox-OM}\left(\frac{gO_2}{L}\right) = 2.857\,\frac{gO_2}{gNO_3^--N}\,(NO_3^--N_{theoretical}-NO_3^--N_{produced}) \tag{8}$$

$$O_{2\,OM}\left(\frac{gO_2}{L}\right) = \left(COD_{influent}-COD_{effluent}\right)-NO_3^--N_{Ox-OM} \tag{9}$$

$$O_{2\,TAN}\left(\frac{gO_2}{L}\right) = 1.831\left(TAN_{influent}-TAN_{effluent}\right) + 3.43\left(NO_2^--N_{effluent}-NO_2^--N_{influent}\right) \tag{10}$$

2.7. Data analysis

The Kendall rank correlation coefficient was used to find the correlation between specific measured parameters. This non-parametric index is recommended for small datasets such as the one in our present study, which was only seven points (Field, 2013). The plotted points only correspond to the correlation coefficients that were significantly different to zero at 95% of confidence.

Principal component analysis (PCA) was computed as a dimensionality reduction method when analysing the trace element concentrations of the analysed WWTPs. To reduce the influence of the naturally different concentrations of the different metals, each set of measured metal concentration was z-scored (average = 0 and standard deviation = 1) before the PCA analysis. The PCA was conducted with the function PCA in MATLAB R2019a, and the results are shown in biplots.

3. Results and discussion

3.1. PN/A streams chemical characterisation

Table 2 shows the (bio)chemical characterisation of the PN/A influent and effluent of the studied WWTPs. Measurements were grouped into descriptors of organic matter (COD, TOC, T. colour and UVA 254), nutrients (PO$_4^{3-}$-P, TP, TAN, NO$_2^-$-N, NO$_3^-$-N, and TN), and conversion capacities (SAOA, SAA and SDA). As shown in Table 2, the WWTP in which THP was implemented (TIL, AME, APE and HEN) showed higher values of COD and TOC in the influents compared with the plants not using THP. Furthermore, the PN/A effluents showed a reduction in the concentration of COD and TOC compared to the influents. The reduction in COD and TOC contents was likely caused by the partial oxidation of the organics in the influents by a heterotrophic consortium of microorganisms, which used the organic matter as carbon and energy sources. In addition, UVA 254 and T. colour followed COD and TOC trends indicating that part of the degraded organics during PN/A corresponded to aromatic and coloured compounds, such as melanoidins. The negligible VFA concentrations in both influent and effluent of the PN/A confirmed that the organic matter in the PN/A reactors did not comprise these AD-intermediates. The occurrence of melanoidins was likely caused by THP before AD as reported by various studies (Barber, 2016; Dwyer et al., 2008b; Zhang, D. et al., 2020).

Non-VFA COD concentrations remained very high in the sludge reject water, indicating that the melanoidins in the PN/A influents were recalcitrant under anaerobic conditions. However, results from our present study clearly indicated that melanoidins were partly biodegradable when exposed to aerobic/anoxic conditions in the PN/A

Table 2
Specific conversion rates related to SAOA, SAA, and SDA in the mixed liquor, and characterisation of the soluble chemical parameters measured in the studied WWTPs.

Microbial activity	SLU-S and SLU-A [a]		OLB		TIL		HEN		APE		AME	
SAOA (g N/g VS/day)	3.9 ± 1.2 (SLU-S)		2.4 ± 0.7		0.2 ± 0.1		0.9 ± 0.5		0.39 ± 0.02		1.10 ± 0.50	
SAA (g N/g VS/day)	1.43 ± 0.07 (SLU-A)		0.91 ± 0.07		0.56 ± 0.04		0.89 ± 0.07		0.89 ± 0.04		0.57 ± 0.08	
SDA (g N/g VS/day)	0.4 ± 0.1 (SLU-A)		0.12 ± 0.03		0.14 ± 0.07		0.23 ± 0.02		0.220 ± 0.013		0.13 ± 0.02	

Soluble parameters	Influent	SHARON Effluent	ANAMMOX Effluent	Influent	Effluent	Influent	Effluent	Influent	Effluent	Influent	Effluent	Influent	Effluent
COD (mg COD/L)	470 ± 17	530 ± 3	314 ± 2	108 ± 2	71 ± 5	3151 ± 5	821 ± 42	3527 ± 20	1874 ± 15	1709 ± 31	811 ± 2	1602 ± 18	1168 ± 6
TOC (mg C/L)	130 ± 5	150 ± 8	107 ± 3	73 ± 4	67.8 ± 0.3	2020 ± 20	296 ± 7	1203 ± 24	685 ± 12	528 ± 3	267 ± 5	506 ± 11	361 ± 10
True colour (mg Pt-Co/L)	236 ± 2	307 ± 9	281 ± 14	701 ± 2	63 ± 24	2563 ± 91	1261 ± 82	5381 ± 55	4891 ± 0	1284 ± 67	1400 ± 52	2260 ± 157	2563 ± 99
UVA 254 (1/cm)	1.075 ± 0.001	2.29 ± 0.04	1.617 ± 0.006	0.261 ± 0.002	0.212 ± 0.005	13.2 ± 0.2	5.1 ± 0.2	22.6 ± 0.2	17.41 ± 0.04	5.58 ± 0.05	4.94 ± 0.01	8.41 ± 0.05	8.04 ± 0.07
SUVA (m·L/mg C)	0.83 ± 0.03	1.52 ± 0.09	1.51 ± 0.04	0.36 ± 0.02	0.313 ± 0.008	0.66 ± 0.01	1.72 ± 0.07	1.88 ± 0.04	2.54 ± 0.05	1.06 ± 0.01	1.85 ± 0.04	1.66 ± 0.04	2.23 ± 0.06
VFA (mg COD/L)	17 ± 16	Not detected	Not detected	Not detected	Not detected	28 ± 7	6 ± 11	70 ± 23	61 ± 2	296 ± 1	16 ± 8	Not detected	Not detected
PO_4^{3-} (mg PO_4^{3-}-P/L) (% of total P)	21.9 ± 0.2 (97%)	27.9 ± 0.2 (91%)	28.3 ± 0.2 (87%)	2.94 ± 0.07 (99%)	18.4 ± 0.2 (99%)	102.6 ± 0.9 (78%)	57 ± 2 (85%)	107 ± 3 (91%)	23 ± 1 (79%)	33.40 ± 0.03 (91%)	172 ± 1 (99%)	29.7 ± 0.5 (92%)	51 ± 6 (97%)
TP mg (P/L)	22.7 ± 0.3	30.9 ± 0.3	32.3 ± 0.2	2.9 ± 0.7	18.61 ± 0.09	131 ± 3	66 ± 2	117 ± 2	29 ± 2	36.7 ± 0.6	175 ± 2	32.3 ± 0.5	52 ± 3
TAN (mg N/L)	1190 ± 119	590 ± 20	55 ± 2	243 ± 19	21.9 ± 2	1970 ± 134	101 ± 8	2400 ± 40	199 ± 3	1663 ± 20	204 ± 0	1910 ± 10	580 ± 22
NO_2^--N (mg N/L)	Not detected	664 ± 7	Not detected	9.76 ± 0.05	1.213 ± 0.006	Not detected	Not detected	Not detected	Not detected	Not detected	Not detected	0.126 ± 0.005	57 ± 2
NO_3^--N (mg N/L)	Not detected	185 ± 22	73.2 ± 0.3	2.5 ± 0.2	23.2 ± 0.4	10.17 ± 0.05	4.0 ± 0.1	17.0 ± 0.2	14.1 ± 0.2	Not detected	Not detected	6.3 ± 0.2	18.4 ± 3
TN (mg N/L)	1399 ± 13	1222 ± 33	136 ± 1	281 ± 17	55 ± 1	2048 ± 140	134 ± 5	2553 ± 42	280 ± 4	1548 ± 33	244 ± 23	2205 ± 32	751 ± 32
EC (mS/cm)	10.45 ± 0.03	6.79 ± 0.01	1.746 ± 0.03	6.35 ± 0.02	4.84 ±	13.50 ± 0.07	2.85 ± 0.01	14.94 ± 0.07	3.61 ± 0.02	13.70 ± 0.07	6.20 ± 0.03	13.54 ± 0.07	5.87 ± 0.03

[a] SLU-S and SLU-A represent Sluisjesdijk Sharon and Anammox reactors, respectively.

reactors. Apparently, the presence of O_2 and/or oxygenated nitrogen compounds like NO_3^- and NO_2^- as the final electron acceptor is of importance to achieve oxidation of these organic compounds. The increased reduction-oxidation (redox) potential under aerobic/anoxic conditions renders a higher potential energy to be harvested by the microorganisms compared to the use of solely organics as final electron acceptors under anaerobic conditions (Aghababaie et al., 2015). Moreover, SUVA increased in the effluents of the PN/A reactors compared to the influents except for the OLB full scale reactor, indicating that effluent organics were characterised by higher aromaticity compared to the influents. The higher aromaticity in the effluents can be explained by microbial preferential consumption of the less aromatic compounds in the influents. Moreover, electrical conductivity decreased in the effluent of all the analysed full-scale plants due to total N removal during the PN/A process.

In contrast to TAN and total N concentrations, PO_4^{3-}-P and TP concentrations did not show clear removal trends in the analysed full-scale plants. In fact, PO_4^{3-}-P and TP showed highly variable concentrations in the studied influents and effluents, ranging from only 2.9 mg P/L (PO_4^{3-}-P in OLB's influent) to 175 mg P/L (TP in APE's effluent). Besides, PO_4^{3-}-P and TP concentrations in the effluents varied independently from the influents' concentrations, increasing in the samples from SLU-S, SLU-A, AME, APE, and OLB. The variable PO_4^{3-}-P concentrations in influent and effluent might be attributed to the presence and activity of PAOs in PN/A reactors. PAOs consume organics (mainly VFA) and release PO_4^{3-}-P under anaerobic conditions, which may. Have occurred when aeration ceased in the PN/A reactors. In contrast, PAOs accumulate PO_4^{3-}-P under oxic/anoxic conditions, decreasing the PO_4^{3-}-P concentration in the reactor broth (Satoh et al., 1992; van Loosdrecht et al., 1997). To the

best of our knowledge, the possible occurrence of simultaneous N and P removal in full-scale PN/A reactors is thus far not reported and needs further research. However, some studies have successfully applied simultaneous P and N removal in lab-scale (Ma et al., 2020; Xu et al., 2019; Zhang, M. et al., 2018). In addition, the PO_4^{3-}-P/TP ratio increased in the effluent of all studied PN/A plants except for HEN, where the concentrations of PO_4^{3-}-P and TP decreased distinctly in the effluent. The change in the PO_4^{3-}-P/TP ratio might be related to melanoidins oxidation with subsequent PO_4^{3-}-P release. The difference between soluble PO_4^{3-}-P and TP concentrations likely corresponded to either PO_4^{3-}-P complexed to the HSs using cations for the chemical binding (Gerke, 1992), or the accumulation of organic-P from microbial metabolites/debris. Additionally, TAN was the predominant N species in the studied PN/A plants' influents, which can be expected treating sludge reject water of the preceding AD process (Table 1). TAN removal efficiencies were exceeding 70% and NO_2^--N was almost not present in all the PN/A effluents of the analysed plants, except for SLU-S. It should be noted that SLU consists of a two-step anammox process where a Sharon reactor is followed by the anammox reactor. Therefore, in SLU-S, NO_2^--N and NO_3^--N increased in the effluent due to TAN oxidation in the Sharon reactor (van Kempen et al., 2001). Also, TN concentrations varied following TAN concentrations, since TN was comprised to a large extent by TAN. Furthermore, NO_3^- occurred in the reactors' effluents as a reaction product, as expected from PN/A stoichiometric conversion (Lotti et al., 2014b). The difference between the sum of TAN, NO_2^--N, NO_3^--N concentrations and the TN concentrations likely corresponded to the soluble organic N fraction, which was a very small fraction. Soluble organic-N in PN/A influents and effluent likely corresponded to N that formed part of the melanoidins structure (Dwyer et al., 2008a; Zhang, D.

et al., 2020).

SAOA, SAA and SDA were assessed to reveal the presence and abundance of the different N converting bacteria and their potential contribution to overall N conversion in the studied PN/A plants. As was expected, SLU-A and SLU-S presented the highest SAOA and SAA (Table 2), since the biomass in the two-step anammox process is largely dominated by one specific type of microorganisms in each reactor. Although denitrification is not pursued in PN/A systems, Table 2 shows that all the analysed plants showed SDA, which was around 25% of the SAA (except for OLB). Remarkably, SLU-A showed the highest SDA, evidencing the occurrence of denitrifiers in the SLU-A reactor; denitrifiers in SLU-A possibly converted NO_3^- into N_2, using organics from microbial decay as electron donor. SAOA was considerably higher compared to SAA in the full-scale plants not using THP. The relatively low SAOA in THP-fed PN/A plants is likely indicative of AOO inhibition caused by the melanoidins and colloidal material present in THP-reject water (Valenzuela-Heredia et al., 2022; Zhang, Q. et al., 2018).

3.2. Stoichiometry of the PN/A reaction and O_2 consumption

Following the PN/A reaction's stoichiometry 7.5 % of TAN-N (molar base) is converted to NO_3^--N as an end-product (Lotti et al., 2014b). Consequently, a lower-than-stoichiometric NO_3^--N concentration in the PN/A effluents indicates NO_3^- reduction. Denitrification and dissimilatory nitrate reduction to ammonia (DNRA) are recognised as the main mechanisms to reduce NO_3^-. Since DNRA only occurs under strict reducing conditions (Pandey et al., 2020), we considered denitrification as the main pathway for NO_3^--N reduction in our present study. Moreover, SDA was observed in all the studied full-scale PN/A reactors (Table 2). The denitrification pathway is enhanced in zones of lower DO, or moderate oxidation-reduction potentials (Rambags et al., 2019), such as the inner part of granules, or in flocs if the aeration is stopped. The latter is prevalent in reactors with intermittent-aeration systems. Fig. 1-a shows a comparison between the stoichiometric NO_3^--N production based on TAN conversion and the difference between the effluent and influent NO_3^--N measured values in mg N/L of each full-scale reactor. The stoichiometric NO_3^--N production was in line with the difference in TAN concentrations in influent and effluent (TAN conversion), which

were distinctly higher in the plants using THP, as has been previously reported (Barber, 2016) and shown in Table 2. Also, the NO_3^--N produced in the PN/A step was close to zero in three out of four of the plants using THP, showing that denitrification consumed all the NO_3^--N generated in PN/A. Conversely, the plants not using THP (SLU and OLB) presented NO_3^--N concentrations close to the stoichiometric production. The proximity between the stoichiometric and measured NO_3^--N values indicated less prominence of denitrification in these full scale PN/A plants. Although considerable SDA values were assessed, the near absence of denitrification was likely due to lack of electron donors such as biodegradable organics. Increased denitrification may increase N_2O formation and thus greenhouse gas emissions, as widely discussed in the literature (Gulhan et al., 2023; Kong et al., 2016; Ma et al., 2017; Massara et al., 2017; Ni and Yuan, 2015). Furthermore, the plants using THP removed more N than stoichiometrically possible via PN/A, indicating that organic matter in the influent was used as electron donor for denitrification. Partially biodegradable organics from THP may have a positive impact on the deammonification process, reducing the N-load to the mainstream nitrification-denitrification process of the WWTP.

The most important control parameter in PN/A systems is DO. Aeration must be controlled carefully to one hand, provide sufficient O_2 to partially oxidise TAN and, on the other hand, to avoid O_2 inhibition of the anammox microorganisms (Morales et al., 2015; Seuntjens et al., 2018). The stoichiometric O_2 demands to oxidise TAN in the influents were calculated and are shown in Fig. 1-b. In the same way as NO_3^--N production, the O_2 demand followed TAN conversion in the influents, and was distinctly higher in the plants using THP due to the elevated TAN concentrations present in the influents. In addition to the required amount of O_2 to convert the TAN into NO_2^--N, an additional amount of O_2 was used to oxidise the organics in the influents (numbers in brackets). The oxidation of organic compounds was likely performed using a combination of O_2, NO_2^--N and NO_3^--N as final electron acceptors, as explained previously. From Fig. 1-b, it can be observed that the additional O_2 demand can reach up to 56 % in the case of TIL, being distinctly higher in the plants using THP. The additional O_2 demand increased the energy requirement of the PN/A reactors, which is primarily dependent on the influent TAN concentration (Deng et al., 2021). It should be noted that AD-reject water is commonly recirculated to the
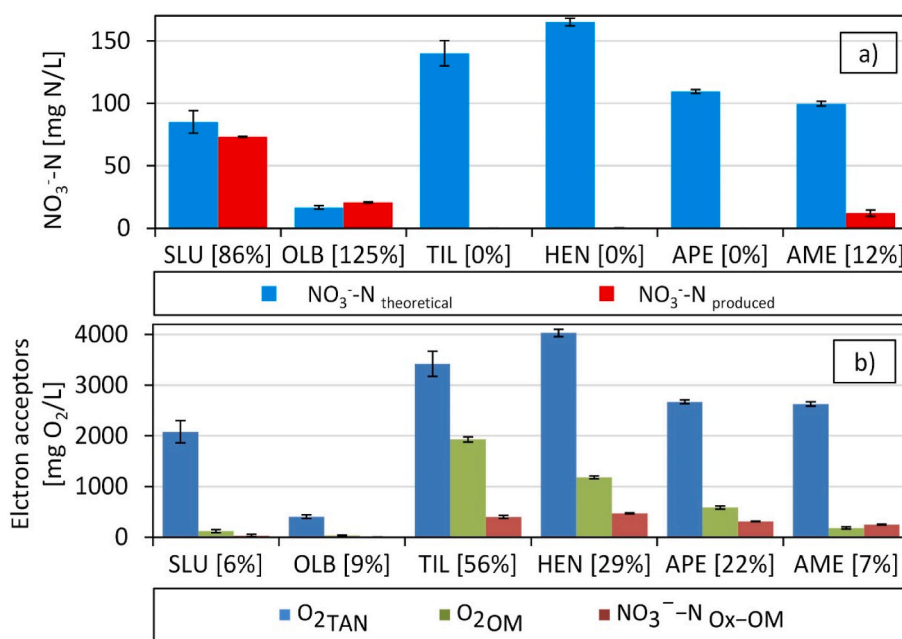

Fig. 1. a) Stoichiometric versus measured NO_3^--N production in the studied plants. The numbers in brackets represent the percentage of NO_3^--N$_{measured}$ over the stoichiometrically produced NO_3^-N; b) Electron acceptors per litre of reactor used to oxidise the TAN and organics in the studied PN/A systems as shown in Equations (8)–(10). The numbers in brackets represent the O_2 used to oxidise organics, over O_2 used to oxidise TAN.
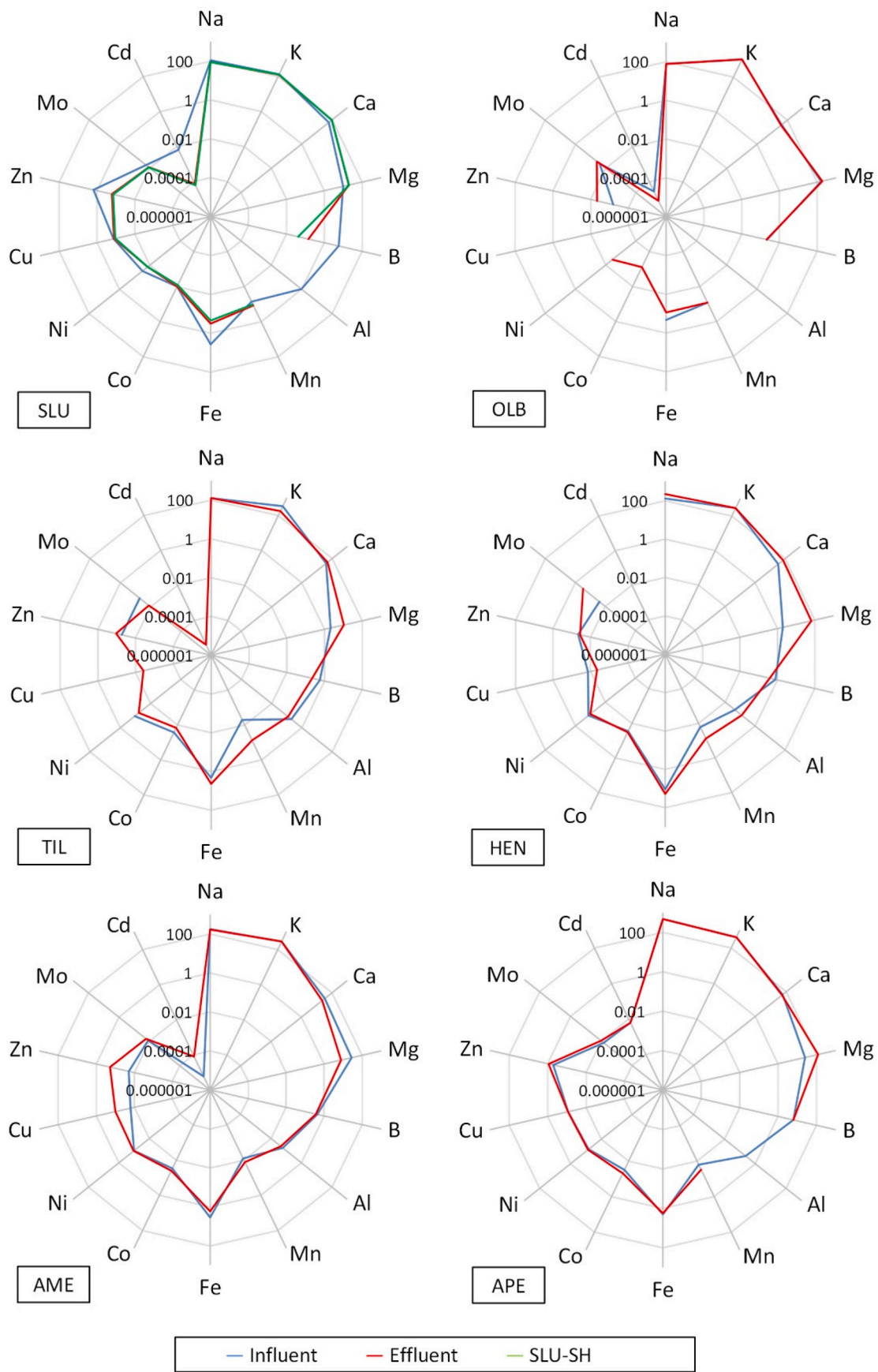
Fig. 2. Cations characterisation in the PN/A step of the studied WWTPs. The units in the vertical axis are mg/L and the scale is logarithmic.

mainstream treatment process for further treatment. This means that in the absence of PN/A, the additional O_2 demand would be otherwise spent in the secondary treatment. However, our results clearly showed that the O_2 demand to mineralise COD (as organics) must also be considered in the process design, even though PN/A systems are commonly designed to only consider the O_2 needed to partially oxidise TAN. The additional O_2 consumption might also affect the required O_2 supply rate, giving additional restrictions to the aeration systems to reach the DO setpoints in the reactors. To verify the influence of THP on the O_2 consumption rate, the O_2 supply and consumption rates must be tested in full-scale reactors and the aeration adapted accordingly.

3.3. PN/A streams trace elements characterisation and complexation assays

Most prevalent cations concentrations were measured in the soluble fraction of the influents and effluents of the studied PN/A reactors using ICP-MS. The cations concentrations are shown in Fig. 2 (full data set available in additional information). It is important to stress that the concentrations of the measured cations differed in all the analysed plants, attributable to the very different treatments applied (Table 1) and the use of specific chemicals in treatment steps prior to PN/A. In some WWTPs, cations were added i) to control process variables such as pH (Na^+ as NaOH); ii) to coagulate/precipitate (in)organic matter (Fe^{3+} as $FeCl_3$); iii) as reagents in previous processes such as Mg^{2+} in struvite precipitation (Abma et al., 2010; Driessen et al., 2020; Oosterhuis et al., 2014).

PCA was conducted as a dimensionality reduction technique to understand the behaviour of the cations present in the influents and effluents of the PN/A reactors analysed (Fig. 3). The variability explained in the two plotted components was 75.8 [%] in the case of the influents and 67.6 [%] in the case of the effluents. Among the influents samples (Fig. 3-a) the data from AME and HEN were the most closely related with 0.04 [RAD] of angle difference among the vectors, followed by TIL with 0.32 [RAD] of difference with HEN. Besides, B, Al, Cu, Zn and Ca were clustered in the two plotted components, while the transition metals Fe, Co Ni and Mo were clustered only in the negative part of the first component. Fig. 3-b shows that SLU-S, SLU-A and OLB behaved similarly, which do not use THP as pre-treatment. Also, HEN and TIL showed similar behaviour. The metals distribution was scattered within the biplot, not showing a clear trend among the metals groups.
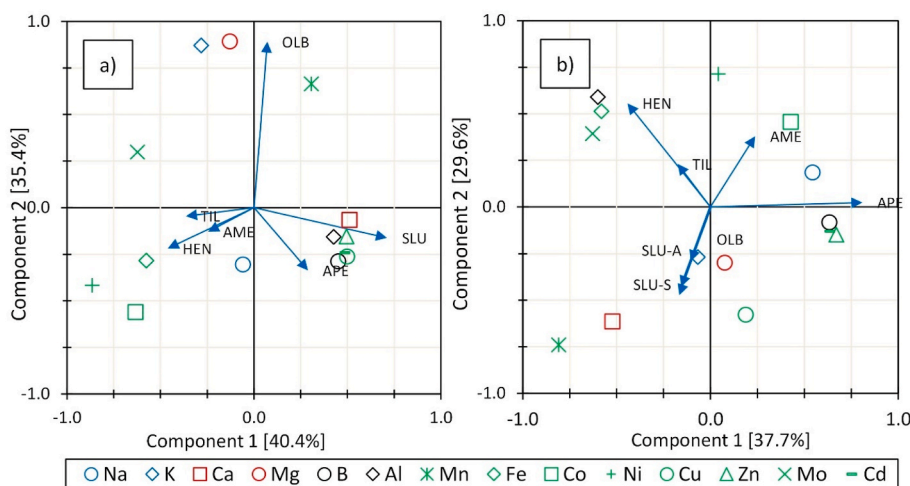

Fig. 4. The fraction of the 0.5 μm filtered supernatant that passed the 1 kDa membrane. The black bars represent the absence of a specific cation in the 0.5 μm filtered supernatant.

3.4. Membrane separation of trace elements in PN/A effluents

HSs and melanoidins behave as multidentate ligands (Mantoura et al., 1978; Tipping, 2002). The metal complexing capacity of these organic compounds can eventually limit the bioavailability of trace elements and hinder microbial growth (anabolism) or substrate conversion capacities (catabolism). Complexation of cations is expected since melanoidins tend to have a negative charge at neutral pH due to the de dissociation of carboxylic and phenolic groups (Bekedam et al., 2008; Migo et al., 1993).

In the plants using THP a maximum of 17% of colour passed the ultrafiltration membrane, which was the case for the APE sample (additional material). The concentrations of trace elements showed a similar pattern as the THP effluent results shown in Fig. 2. The observed high similarity in results was likely caused by the used membranes in the filtration processes having a similar pore size, viz. The dead-end filtration membrane had a pore size of 0.45 μm (data in Fig. 2) and the crossflow filtration membrane had a pore size of 0.5 μm (Fig. 4).

Fig. 4 shows the cation fractions that were filtered using a 0.5 μm pore size membrane and subsequently passed the 1 kDa ultrafiltration membrane. A low value in the 1 kDa-filtered fraction implies that the specific cation is to a great extent complexed to the melanoidins present in the broth of PN/A reactors. Results in Fig. 4 show that Al was strongly complexed by the melanoidins in the broth, since Al was nearly absent in the 1 kDa permeate. Furthermore, Al was not found at all in three of the 0.5 μm filtered effluents (Fig. 5, black bars), likely because it formed part of the

Fig. 3. PCA of the cations analysed in PN/A reactors of the studied plants. Cations are clustered and indicated with different colours: blue = monovalent; red = divalent; black: trivalent (metalloids); multivalent (transition metals). (For interpretation of the references to colour in this figure legend, the reader is referred to the Web version of this article.)
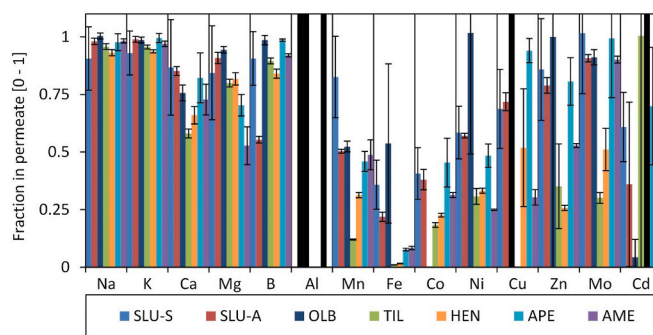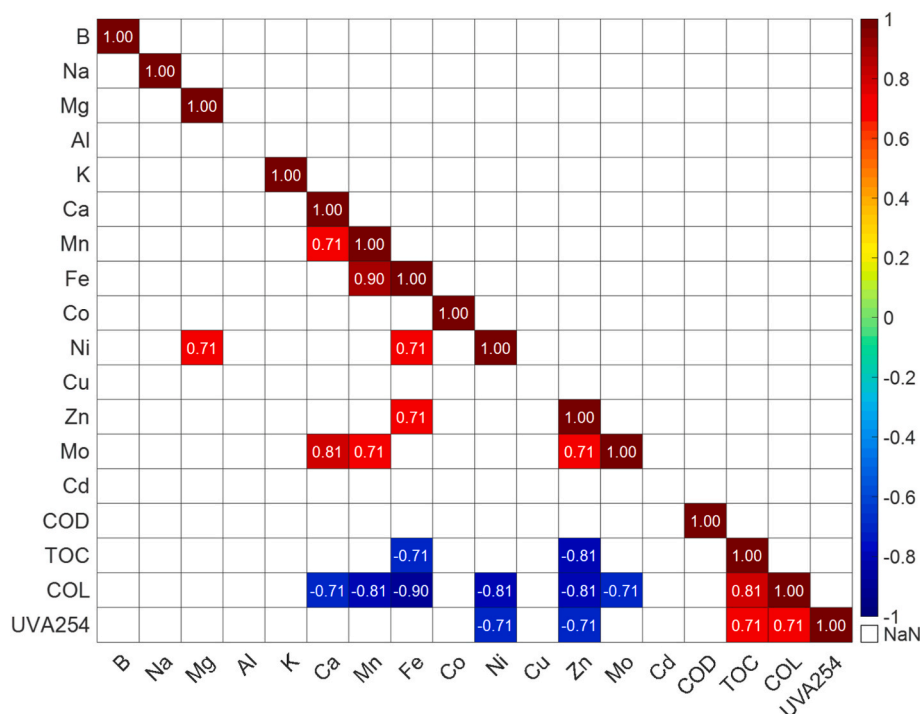
Fig. 5. Significant correlation at 95% of confidence of Kendall correlation coefficient (τ) between the concentration of COD, TOC, COL, and UVA 254 in the 0.5 μm fraction, and the fraction of cations that passed through the 1 kDa membrane.

solids and colloidal matrix and was thus rejected by the 0,5 μm membrane. The binding capacity of Al with organics is widely reported in various concentrations and pHs (Tipping et al., 1988). Next to Al, Fe was the second element in place regarding the degree of complexation with melanoidins, showing an average of only 19% of the Fe fraction that passed the 1 kDa membrane (Fig. 4). Notably, compared to the THP equipped full-scale plants, larger Fe fractions in the 1 kDa permeates were measured in the plants not using THP, reaching 36%, 22% and 54% in the case of SLU-S, SLU-A and OLB, respectively. In all the plants using THP as pre-treatment and which were characterised by relatively high concentrations of organic matter (Table 2), the observed Fe complexation was considerable. The fractions that passed the 1 kDa membrane reached only 1%, 8%, 8%, and 2% in the case of TIL, AME, APE, and HEN, respectively (Fig. 4). We, therefore, hypothesize that the effects of THP on Fe concentration in the 1 kDa permeates was indicative for the complexation of this metal with the THP-created melanoidins. Fe commonly occurs in biological systems in oxidation states Fe^{2+} and Fe^{3+}, and the specific oxidation state mainly depends on the redox conditions (Pehkonen, 1995). After AD, Fe is expected to occur in reject waters in the reduced form (Fe^{2+}). However, during struvite precipitation, which is commonly performed in airlift reactors, and in limitedly aerated PN/A reactors, Fe^{2+} is likely oxidised to Fe^{3+}. The Fe^{3+} ion strongly binds HSs, forming stable bonds with multidentate ligands, such as HSs and melanoidins (Srivastva, 2020). Fe is an important metal in the anammox heme proteins, which constitute up to 30% of the protein content and gives these microorganisms their distinctive reddish colour (Ferousi et al., 2017; Kartal et al., 2012). In addition, Fe is involved in NH_4^+ oxidation, being part of the ammonium-monooxygenase metalloenzyme. Ammonium-monooxygenase catalyses the conversion of NH_4^+ to hydroxylamine (Gilch et al., 2009).

Also, Mn and Co were strongly complexed with melanoidins, and less than 50% of these metals passed through the 1 kDa membrane. Co is an essential nutrient for microbial growth involved in the N-cycle (Nicholas et al., 1964). Co has also shown positive effects on the anammox conversion capacity when dosed as a trace element (Li et al., 2020). Furthermore, Ni can be found in metalloproteins produced by some AOO, such as urease (Koper et al., 2004). However, Ni can be toxic if

present in high concentrations, with IC_{50} values of 6.0 mg Ni/L in solution (Kalkan Aktan et al., 2018) that were never reached in our present study.

The cations' complexation stability depends on many factors such as oxidation state, atomic radius and nature of the ligands; however, they follow the Irving–Williams series for divalent cations (Mn < Fe < Co < Ni < Cu > Zn) (Irving and Williams, 1953). The complexation of specific trace elements that play a role in enzymatic cofactors may hinder both, microbial catabolism, and anabolism in PN/A biomass from full-scale installations using THP.

3.5. Correlation analysis of cation complexation and organic matter in the PN/A reactors

A correlation analysis was performed among the fraction of metals that passed the 1 kDa membrane (non-complexed) and the melanoidins indicators such as COD, TOC, COL, and UVA 254 in the 0.5 μm fraction of PN/A. The Kendall correlation coefficient (τ) was calculated; this coefficient is employed for non-parametric correlations in small datasets, which was only seven data points in this case (Field, 2013). Also, a two-tailed ANOVA analysis at 95% of confidence was performed to analyse the correlation significance. Fig. 5 shows significant correlations at 95% of confidence of τ between the parameters, COD, TOC, COL, and UVA 254, in the 0.5 μm fraction, and the fraction of cations that passed the 1 kDa membrane. A negative correlation coefficient means that the cation was more HSs-complexed and hence, less bioavailable. Fig. 5 shows that the largest negative correlation was found between Fe and colour ($\tau = 0.90$). This highly negative correlation showed that the increased concentration of colour in the broth of PN/A reactors produced a higher extent of complexed Fe. Also, colour presented a negative correlation coefficient with Mn, Ni, and Zn ($\tau = 0.81$), which indicated a high complexation of these metals with HSs that caused colour occurrence. Furthermore, UVA 254 presented a significantly negative correlation coefficient with Ni and Zn, and TOC with Fe and Zn. Overall, colour in the PN/A effluents showed a significant negative correlation coefficient with the chelation of six multivalent cations (Ca, Mn, Fe, Ni,

Zn and Mo). These results showed that the complexation of cations in the effluents of PN/A reactors was correlated with the melanoidins occurrence. Our present study proved that the complexation of cations with multidentate ligands occurred, which eventually may cause problems in full-scale PN/A reactors. However, current results did not prove any biomass growth/conversion-rate limitation as a consequence of trace elements scarcity. To identify the trace elements that indeed limit bioconversion, further research is needed in the field of trace elements availability in biological systems with high concentrations of polydentate ligands.

3.6. Significance of the results for full-scale installations using THP

The increased TAN and melanoidin concentrations associated with AD-THP, demand optimized operational parameters and control strategies. In full-scale PN/A reactors that are not designed for elevated concentrations of organics and TAN, some modifications are required. DO control systems need to be adjusted to the elevated O_2 consumption rate, due to the degradation of biodegradable organics. Fulfilling the increased O_2 requirements could be reached by extending the aeration periods in intermittent aeration systems, or installing additional aeration systems. Also, the TAN conversion capacity likely needs to be increased, which can be attained by increasing the concentration of AOO in the reactors or extending the retention time in the reactors. Increase in AOO concentration may be reached by improving the liquid solids separation techniques as used in DEMON® systems (Izadi et al., 2021).

Elevated denitrification capacity in PN/A systems has the potential to enhance the N-removal efficiency from the reject waters. However, it also raises concerns regarding increased greenhouse gas emissions, such as N_2O. Further studies are needed to understand N_2O emissions from the treatment of reject water from AD-THP-based systems.

Transition metals-melanoidins complexation was discussed as a side-effect of the use of reject water from a THP-AD system. Trace metals complexation might cause trace elements limitation in the PN/A microbial populations. Future research is needed to explore the effects of specific trace metal limitations and its implications for microbial PN/A populations. Full-scale mitigation strategies, such as trace elements addition to PN/A systems, may help to alleviate metals limitation in the case of PN/A systems working with high concentrations of melanoidins.

4. Conclusions

The analysis of the studied PN/A systems allowed us to draw the following conclusions:

- The use of THP as AD pre-treatment technique, increased COD, TOC, T. colour and UVA 254 in influents of PN/A systems, evidencing an increase in the concentrations of melanoidins in full-scale PN/A systems. The melanoidins in the PN/A influents were not fully recalcitrant under the aerobic/anoxic conditions, and were partly degraded during the PN/A step.
- The use of AD-THP increased the O_2 requirements in the PN/A reactors, which resulted in increased aeration requirements in full-scale installations. The additional O_2 was used to oxidise the elevated concentrations of TAN and non-recalcitrant melanoidins in PN/A influents.
- In WWTPs using AD-THP, NO_3^--N concentrations in PN/A effluents were lower than the stoichiometric values, attributable to the occurrence of heterotrophic denitrification. Denitrifying microorganisms using the organic matter in the reject waters as electron donors, increased the N-removal efficiency in PN/A systems treating AD-THP reject waters.
- The presence of melanoidins in the effluents of PN/A reactors increased the fraction of chelated Fe and other transition metals. The complexation of transition metals in PN/A effluents is mainly correlated with the presence and intensity of colour. The

complexation of transition metals might cause trace metals limitation in the microbial populations of the PN/A systems.

Contributions

Javier A. Pavez-Jara: Conceptualization, data curation, formal analysis, funding acquisition, investigation, methodology, resources, software, validation, visualization, writing – original draft, writing – review & editing; **Jules B. van Lier**: Formal analysis, funding acquisition, project administration, resources, supervision, writing – review & editing; **Merle K. de Kreuk**: Conceptualization, funding acquisition, project administration, resources, supervision, writing – review & editing.

Declaration of competing interest

The authors declare the following financial interests/personal relationships which may be considered as potential competing interests: Merle de Kreuk reports financial support was provided by Top Consortia for Knowledge and Innovation. Jules van Lier reports financial support was provided by Foundation for Applied Water Research. Javier Pavez reports financial support was provided by National Agency for Research and Development.

Data availability

Data will be made available on request.

Acknowledgements

Appendix A. Supplementary data

Supplementary data to this article can be found online at https://doi.org/10.1016/j.jclepro.2023.139767.

Abbreviations

AD	anaerobic digestion
AME	Amersfoort
AOO	aerobic ammonium oxidising organisms
APE	Apeldoorn
COD	chemical oxygen demand.
DNRA	dissimilatory nitrate reduction to ammonia
DO	dissolved oxygen
EC	electroconductivity
FAN	free ammonia nitrogen
FID-GC	flame ionisation detector gas chromatography
HEN	Hengelo
HSs	humic substances
OLB	Olburgen
PCA	principal component analysis
PN/A	partial nitritation/anammox
SAA	specific anammox activity
SAOA	specific ammonium oxidising activity
SDA	specific denitrifying activity
SLU	Sluisjesdijk

SUVA	specific ultraviolet absorbance
T. colour	True colour
TAN	total ammoniacal nitrogen
THP	thermal hydrolysis process
TIL:	Tilburg
TN	total nitrogen
TOC	total organic carbon
TP	Total phosphorous
TS	Total solids
UVA 254	ultraviolet absorbance at 254 nm
VFA	volatile fatty acids
VS	volatile solids
WAS	waste activated sludge
WWTPs	wastewater treatment plants
τ	Kendall correlation coefficient

References

Abma, W.R., Driessen, W., Haarhuis, R., van Loosdrecht, M.C.M., 2010. Upgrading of sewage treatment plant by sustainable and cost-effective separate treatment of industrial wastewater. Water Sci. Technol. 61 (7), 1715–1722.

Aghababaie, M., Farhadian, M., Jeihanipour, A., Biria, D., 2015. Effective factors on the performance of microbial fuel cells in wastewater treatment – a review. Environmental Technology Reviews 4 (1), 71–89.

Appels, L., Baeyens, J., Degrève, J., Dewil, R., 2008. Principles and potential of the anaerobic digestion of waste-activated sludge. Prog. Energy Combust. Sci. 34 (6), 755–781.

Baeten, J.E., Batstone, D.J., Schraa, O.J., van Loosdrecht, M.C.M., Volcke, E.I.P., 2019. Modelling anaerobic, aerobic and partial nitration-anammox granular sludge reactors - a review. Water Res. 149, 322–341.

Barber, W.P.F., 2016. Thermal hydrolysis for sewage treatment: a critical review. Water Res. 104, 53–71.

Becker, G.C., Wüst, D., Köhler, H., Lautenbach, A., Kruse, A., 2019. Novel approach of phosphate-reclamation as struvite from sewage sludge by utilising hydrothermal carbonization. J. Environ. Manag. 238, 119–125.

Bekedam, E.K., Roos, E., Schols, H.A., Van Boekel, M.A.J.S., Smit, G., 2008. Low molecular weight melanoidins in coffee brew. J. Agric. Food Chem. 56 (11), 4060–4067.

Bougrier, C., Delgenès, J.P., Carrère, H., 2008. Effects of thermal treatments on five different waste activated sludge samples solubilisation, physical properties and anaerobic digestion. Chem. Eng. J. 139 (2), 236–244.

Ceron-Chafla, P., Kleerebezem, R., Rabaey, K., van Lier, J.B., Lindeboom, R.E.F., 2020. Direct and indirect effects of increased CO2 partial pressure on the bioenergetics of syntrophic propionate and butyrate conversion. Environ. Sci. Technol. 54 (19), 12583–12592.

Coats, E.R., Watkins, D.L., Kranenburg, D., 2011. A comparative environmental life-cycle analysis for removing phosphorus from wastewater: biological versus physical/chemical processes. Water Environ. Res. 83 (8), 750–760.

Deng, Z., van Linden, N., Guillen, E., Spanjers, H., van Lier, J.B., 2021. Recovery and applications of ammoniacal nitrogen from nitrogen-loaded residual streams: a review. J. Environ. Manag. 295, 113096.

Devos, P., Filali, A., Grau, P., Gillot, S., 2023. Sidestream characteristics in water resource recovery facilities: a critical review. Water Res. 232, 119620.

Driessen, W., Van Veldhoven, J.T.A., Janssen, M.P.M., Van Loosdrecht, M.C.M., 2020. Treatment of sidestream dewatering liquors from thermally hydrolised and anaerobically digested biosolids. Water Pract. Technol. 15 (1), 142–150.

Dwyer, J., Kavanagh, L., Lant, P., 2008a. The degradation of dissolved organic nitrogen associated with melanoidin using a UV/H2O2 AOP. Chemosphere 71 (9), 1745–1753.

Dwyer, J., Starrenburg, D., Tait, S., Barr, K., Batstone, D.J., Lant, P., 2008b. Decreasing activated sludge thermal hydrolysis temperature reduces product colour, without decreasing degradability. Water Res. 42 (18), 4699–4709.

El-sayed, M.E., Abdelaal, W.A., Ahmed, A.A., 2017. Effect of using treated drainage water by modified clay on some plant and soil properties. Nat. Sci. 15 (12), 17–25.

Ferousi, C., Lindhoud, S., Baymann, F., Kartal, B., Jetten, M.S.M., Reimann, J., 2017. Iron assimilation and utilization in anaerobic ammonium oxidizing bacteria. Curr. Opin. Chem. Biol. 37, 129–136.

Field, A., 2013. Discovering Statistics Using IBM SPSS Statistics. sage.

Fischer, F., Bastian, C., Happe, M., Mabillard, E., Schmidt, N., 2011. Microbial fuel cell enables phosphate recovery from digested sewage sludge as struvite. Bioresour. Technol. 102 (10), 5824–5830.

Flores-Alsina, X., Solon, K., Kazadi Mbamba, C., Tait, S., Gernaey, K.V., Jeppsson, U., Batstone, D.J., 2016. Modelling phosphorus (P), sulfur (S) and iron (Fe) interactions for dynamic simulations of anaerobic digestion processes. Water Res. 95, 370–382.

Fux, C., Siegrist, H., 2004. Nitrogen removal from sludge digester liquids by nitrification/denitrification or partial nitration/anammox: environmental and economical considerations. Water Sci. Technol. 50 (10), 19–26.

Gerke, J., 1992. Orthophosphate and organic phosphate in the soil solution of four sandy soils in relation to pH-evidence for humic-FE-(AL-) phosphate complexes. Commun. Soil Sci. Plant Anal. 23 (5–6), 601–612.

Gilbert, E.M., Müller, E., Horn, H., Lackner, S., 2013. Microbial activity of suspended biomass from a nitration–anammox SBR in dependence of operational condition and size fraction. Appl. Microbiol. Biotechnol. 97 (19), 8795–8804.

Gilch, S., Meyer, O., Schmidt, I., 2009. A soluble form of ammonia monooxygenase in Nitrosomonas europaea 390 (9), 863–873.

Gulhan, H., Cosenza, A., Mannina, G., 2023. Modelling greenhouse gas emissions from biological wastewater treatment by GPS-X: the full-scale case study of Corleone (Italy). Sci. Total Environ. 905, 167327.

Hendriks, A.T.W.M., Zeeman, G., 2009. Pretreatments to enhance the digestibility of lignocellulosic biomass. Bioresour. Technol. 100 (1), 10–18.

Hodge, J.E., 1953. Dehydrated foods, chemistry of browning reactions in model systems. J. Agric. Food Chem. 1 (15), 928–943.

Irving, H., Williams, R., 1953. 637. The stability of transition-metal complexes. J. Chem. Soc. 3192–3210.

Izadi, P., Izadi, P., Eldyasti, A., 2021. Towards mainstream deammonification: comprehensive review on potential mainstream applications and developed sidestream technologies. J. Environ. Manag. 279, 111615.

Joss, A., Salzgeber, D., Eugster, J., König, R., Rottermann, K., Burger, S., Fabijan, P., Leumann, S., Mohn, J., Siegrist, H., 2009. Full-scale nitrogen removal from digester liquid with partial nitration and anammox in one SBR. Environ. Sci. Technol. 43 (14), 5301–5306.

Kalkan Aktan, C., Uzunhasanoglu, A.E., Yapsakli, K., 2018. Speciation of nickel and zinc, its short-term inhibitory effect on anammox, and the associated microbial community composition. Bioresour. Technol. 268, 558–567.

Kartal, B., van Niftrik, L., Keltjens, J.T., Op den Camp, H.J.M., Jetten, M.S.M., 2012. Chapter 3 - anammox—growth physiology, cell biology, and metabolism. In: Poole, R.K. (Ed.), Advances in Microbial Physiology. Academic Press, pp. 211–262.

Kong, Q., Wang, Z.-b., Niu, P.-f., Miao, M.-s., 2016. Greenhouse gas emission and microbial community dynamics during simultaneous nitrification and denitrification process. Bioresour. Technol. 210, 94–100.

Koper, T.E., El-Sheikh, A.F., Norton, J.M., Klotz, M.G., 2004. Urease-encoding genes in ammonia-oxidizing bacteria. Appl. Environ. Microbiol. 70 (4), 2342–2348.

Kor-Bicakci, G., Eskicioglu, C., 2019. Recent developments on thermal municipal sludge pretreatment technologies for enhanced anaerobic digestion. Renew. Sustain. Energy Rev. 110, 423–443.

L. Malcolm, R., 1990. The uniqueness of humic substances in each of soil, stream and marine environments. Anal. Chim. Acta 232, 19–30.

Lackner, S., Gilbert, E.M., Vlaeminck, S.E., Joss, A., Horn, H., van Loosdrecht, M.C.M., 2014. Full-scale partial nitration/anammox experiences – an application survey. Water Res. 55, 292–303.

Li, J., Chen, X., Liu, W., Tao, Y., 2020. Biostimulation of a marine anammox bacteria-dominated bioprocess by Co(II) to treat nitrogen-rich, saline wastewater. Sci. Total Environ. 749, 141489.

Li, Y.-Y., Noike, T., 1992. Upgrading of anaerobic digestion of waste activated sludge by thermal pretreatment. Water Sci. Technol. 26 (3–4), 857–866.

Lotti, T., Kleerebezem, R., Hu, Z., Kartal, B., Jetten, M.S.M., van Loosdrecht, M.C.M., 2014a. Simultaneous partial nitration and anammox at low temperature with granular sludge. Water Res. 66, 111–121.

Lotti, T., Kleerebezem, R., Lubello, C., van Loosdrecht, M.C.M., 2014b. Physiological and kinetic characterization of a suspended cell anammox culture. Water Res. 60, 1–14.

Ma, C., Jensen, M.M., Smets, B.F., Thamdrup, B., 2017. Pathways and controls of N2O production in nitration–anammox biomass. Environ. Sci. Technol. 51 (16), 8981–8991.

Ma, H., Xue, Y., Zhang, Y., Kobayashi, T., Kubota, K., Li, Y.-Y., 2020. Simultaneous nitrogen removal and phosphorus recovery using an anammox expanded reactor operated at 25 °C. Water Res. 172, 115510.

Mantoura, R.F.C., Dickson, A., Riley, J.P., 1978. The complexation of metals with humic materials in natural waters. Estuar. Coast Mar. Sci. 6 (4), 387–408.

Massara, T.M., Malamis, S., Guisasola, A., Baeza, J.A., Noutsopoulos, C., Katsou, E., 2017. A review on nitrous oxide (N2O) emissions during biological nutrient removal from municipal wastewater and sludge reject water. Sci. Total Environ. 596–597, 106–123.

McDonald, S., Bishop, A.G., Prenzler, P.D., Robards, K., 2004. Analytical chemistry of freshwater humic substances. Anal. Chim. Acta 527 (2), 105–124.

Migo, V.P., Matsumura, M., Del Rosario, E.J., Kataoka, H., 1993. The effect of pH and calcium ions on the destabilization of melanoidin. J. Ferment. Bioeng. 76 (1), 29–32.

Morales, F.J., Fernández-Fraguas, C., Jiménez-Pérez, S., 2005. Iron-binding ability of melanoidins from food and model systems. Food Chem. 90 (4), 821–827.

Morales, N., Val del Río, A., Vázquez-Padín, J.R., Gutiérrez, R., Fernández-González, R., Icaran, P., Rogalla, F., Campos, J.L., Méndez, R., Mosquera-Corral, A., 2015. Influence of dissolved oxygen concentration on the start-up of the anammox-based process: ELAN®. Water Sci. Technol. 72 (4), 520–527.

Ni, B.-J., Yuan, Z., 2015. Recent advances in mathematical modeling of nitrous oxides emissions from wastewater treatment processes. Water Res. 87, 336–346.

Nicholas, D.J.D., Fisher, D.J., Redmond, W.J., Osborne, M., 1964. A cobalt requirement for nitrogen fixation, hydrogenase, nitrite and hydroxylamine reductases in clostridium pasteurianum. Nature 171 (4921), 793–795.

Ødeby, T., Netteland, T., Solheim, O.E., 1996. Thermal hydrolysis as a profitable way of handling sludge. In: Hahn, H.H., Hoffmann, E., Ødegaard, H. (Eds.), Chemical Water and Wastewater Treatment IV. Springer Berlin Heidelberg, Berlin, Heidelberg, pp. 401–409.

Oosterhuis, M., Ringoot, D., Hendriks, A., Roeleveld, P., 2014. Thermal hydrolysis of waste activated sludge at hengelo wastewater treatment plant, The Netherlands. Water Sci. Technol. 70 (1), 1–7.

Pandey, C.B., Kumar, U., Kaviraj, M., Minick, K.J., Mishra, A.K., Singh, J.S., 2020. DNRA: a short-circuit in biological N-cycling to conserve nitrogen in terrestrial ecosystems. Sci. Total Environ. 738, 139710.

Pavlostathis, S., Giraldo-Gomez, E., 1991. Kinetics of anaerobic treatment: a critical review. Crit. Rev. Environ. Sci. Technol. 21 (5–6), 411–490.

Pehkonen, S., 1995. Determination of the oxidation states of iron in natural waters. A review. Analyst 120 (11), 2655–2663.

Penaud, V., Delgenès, J.-P., Moletta, R., 2000. Characterization of soluble molecules from thermochemically pretreated sludge. J. Environ. Eng. 126 (5), 397–402.

Qiu, G., Zuniga-Montanez, R., Law, Y., Thi, S.S., Nguyen, T.Q.N., Eganathan, K., Liu, X., Nielsen, P.H., Williams, R.B.H., Wuertz, S., 2019. Polyphosphate-accumulating organisms in full-scale tropical wastewater treatment plants use diverse carbon sources. Water Res. 149, 496–510.

Rambags, F., Tanner, C.C., Schipper, L.A., 2019. Denitrification and anammox remove nitrogen in denitrifying bioreactors. Ecol. Eng. 138, 38–45.

Rice, E.W., Baird, R.B., Eaton, A.D., Clesceri, L.S., 2012. Standard Methods for the Examination of Water and Wastewater. American Public Health Association, Washington, DC.

Ringoot, D., Kleiven, H., Panter, K., 2012. Energy efficient thermal hydrolysis with steam explosion. In: 17th European Biosolids and Organic Resources Conference Abstract, pp. 1–8.

Satoh, H., Mino, T., Matsuo, T., 1992. Uptake of organic substrates and accumulation of polyhydroxyalkanoates linked with glycolysis of intracellular carbohydrates under anaerobic conditions in the biological excess phosphate removal processes. Water Sci. Technol. 26 (5–6), 933–942.

Seuntjens, D., Carvajal-Arroyo, J.M., Ruopp, M., Bunse, P., De Mulder, C.P., Lochmatter, S., Agrawal, S., Boon, N., Lackner, S., Vlaeminck, S.E., 2018. High-resolution mapping and modeling of anammox recovery from recurrent oxygen exposure. Water Res. 144, 522–531.

Srivastva, A.N., 2020. Stability and Applications of Coordination Compounds. BoD–Books on Demand.

Strous, M., Heijnen, J.J., Kuenen, J.G., Jetten, M.S.M., 1998. The sequencing batch reactor as a powerful tool for the study of slowly growing anaerobic ammonium-oxidizing microorganisms. Appl. Microbiol. Biotechnol. 50 (5), 589–596.

Tiehm, A., Nickel, K., Zellhorn, M., Neis, U., 2001. Ultrasonic waste activated sludge disintegration for improving anaerobic stabilization. Water Res. 35 (8), 2003–2009.

Tipping, E., 2002. Cation Binding by Humic Substances. Cambridge University Press.

Tipping, E., Woof, C., Backes, C.A., Ohnstad, M., 1988. Aluminium speciation in acidic natural waters: testing of a model for al-humic complexation. Water Res. 22 (3), 321–326.

Valenzuela-Heredia, D., Panatt, C., Belmonte, M., Franchi, O., Crutchik, D., Dumais, J., Vázquez-Padín, J.R., Lesty, Y., Pedrouso, A., Val del Río, Á., Mosquera-Corral, A.,

Campos, J.L., 2022. Performance of a two-stage partial nitration-anammox system treating the supernatant of a sludge anaerobic digester pretreated by a thermal hydrolysis process. Chem. Eng. J. 429, 131301.

Van Hulle, S.W.H., Vandeweyer, H.J.P., Meesschaert, B.D., Vanrolleghem, P.A., Dejans, P., Dumoulin, A., 2010. Engineering aspects and practical application of autotrophic nitrogen removal from nitrogen rich streams. Chem. Eng. J. 162 (1), 1–20.

van Kempen, R., Mulder, J.W., Uijterlinde, C.A., Loosdrecht, M.C.M., 2001. Overview: full scale experience of the SHARON® process for treatment of rejection water of digested sludge dewatering. Water Sci. Technol. 44 (1), 145–152.

van Loosdrecht, M.C.M., Hooijmans, C.M., Brdjanovic, D., Heijnen, J.J., 1997. Biological phosphate removal processes. Appl. Microbiol. Biotechnol. 48 (3), 289–296.

Wang, H.-Y., Qian, H., Yao, W.-R., 2011. Melanoidins produced by the Maillard reaction: structure and biological activity. Food Chem. 128 (3), 573–584.

Wang, R., Li, Y., Chen, W., Zou, J., Chen, Y., 2016. Phosphate release involving PAOs activity during anaerobic fermentation of EBPR sludge and the extension of ADM1. Chem. Eng. J. 287, 436–447.

Wang, W., Xie, H., Wang, H., Xue, H., Wang, J., Zhou, M., Dai, X., Wang, Y., 2020. Organic compounds evolution and sludge properties variation along partial nitritation and subsequent anammox processes treating reject water. Water Res. 184, 116197.

Xu, X., Qiu, L., Wang, C., Yang, F., 2019. Achieving mainstream nitrogen and phosphorus removal through Simultaneous partial Nitrification, Anammox, Denitrification, and Denitrifying Phosphorus Removal (SNADPR) process in a single-tank integrative reactor. Bioresour. Technol. 284, 80–89.

Yuan, Z., Pratt, S., Batstone, D.J., 2012. Phosphorus recovery from wastewater through microbial processes. Curr. Opin. Biotechnol. 23 (6), 878–883.

Zhang, D., Feng, Y., Huang, H., Khunjar, W., Wang, Z.-W., 2020. Recalcitrant dissolved organic nitrogen formation in thermal hydrolysis pretreatment of municipal sludge. Environ. Int. 138, 105629.

Zhang, M., Qiao, S., Shao, D., Jin, R., Zhou, J., 2018. Simultaneous nitrogen and phosphorus removal by combined anammox and denitrifying phosphorus removal process. J. Chem. Technol. Biotechnol. 93 (1), 94–104.

Zhang, Q., Vlaeminck, S.E., DeBarbadillo, C., Su, C., Al-Omari, A., Wett, B., Pümpel, T., Shaw, A., Chandran, K., Murthy, S., De Clippeleir, H., 2018. Supernatant organics from anaerobic digestion after thermal hydrolysis cause direct and/or diffusional activity loss for nitritation and anammox. Water Res. 143, 270–281.

Zhang, T., He, X., Deng, Y., Tsang, D.C.W., Yuan, H., Shen, J., Zhang, S., 2020. Swine manure valorization for phosphorus and nitrogen recovery by catalytic–thermal hydrolysis and struvite crystallization. Sci. Total Environ. 729, 138999.